Acta Geologica Sinica (English Edition), 2020, 94(3): 777–788

Geochemical Aspects of Hypogene Hydrothermal Alteration Zones in the Chol-qeshlaghi Area, NW Iran: Constrains on REEs

Kamal SIAHCHESHM* and Mohammad SHAHSAVANI BAMI

Department of Earth Sciences, University of Tabriz, Tabriz, Iran 5166616471

Abstract: Chol-qeshlaghi altered area lies in the northwestern part of the post-collisional Urumieh-Dokhtar magmatic arc, NW Iran. Pervasive silicic, argillic, phyllic and propylitic altered zones appears to be intimately affiliated to the fluids derivative of upper Oligocene Khankandi granodiorite. This paper is dedicated to the identification of geochemical characteristics of hydrothermal alterations, focusing on the determination of the mass gains and losses of REEs, to gain significant insights regarding the chemical exchanges prevailed between the host rocks and hydrothermal fluids. The low pH and high activity of SO_4^{-2} ligands in silicic alteration fluids, resulting in depletion of entire REEs. Decreasing of LREEs appeared in argillic zone may attributed to reduce in adsorption ability of clay minerals in low pH; whereas HREEs enrichment in phyllic zone was inclined to put it down to the abundance of sericite (± Fe oxides). A significant reduction of Eu/Eu* ratio in silicic zone can be attributed to negligible sulfides and clay minerals as some effective agents in adsorption of released Eu^{+2}. Factors such as changes in pH, the abundance of absorptive neomorph mineral phases, activity of ligands play an important role in controlling the distribution and concentration of REEs in Chol-qeshlaghi alteration system.

Key words: argillic alteration, rare earth elements, Eu/Eu* ratio, Chol-qeshlaghi

Citation: Siahcheshm and Shahsavani Bami, 2020. Geochemical Aspects of Hypogene Hydrothermal Alteration Zones in the Chol-qeshlaghi Area, NW Iran: Constrains on REEs. Acta Geologica Sinica (English Edition), 94(3): 777–788. DOI: 10.1111/1755-6724.13885

1 Introduction

Qaradagh metallogenic district, in the southern Lesser Caucasus, NW Iran, is considered as a part of the larger Tethyan-Eurasian metallogenic belt which was formed during Mesozoic and Early Cenozoic times (Jankovi´c, 1997). After the closure of the Neo-Tethys, mineralization and/or alteration in this district was controlled by extensional events related to Oligo-Miocene calc-alkaline magmatic activity during post collisional, slab breakoff-induced heat and fluid flow from upwelling asthenosphere beneath the young orogenic belt (Aghazadeh et al., 2011; Siahcheshm, 2017). The intrusive suites are mainly lens-shaped characterized by variable age, size, and composition. The hypabyssal upper -Oligocene plutonic rocks are generally associated with extensive porphyry Cu-(-Au-Mo) mineralization, representing Tertiary metallogenic episodes in the Qaradagh district. It hosts many porphyry copper deposits (PCDs) [e.g., Sungun Cu-Mo:Calagari, 2004; Masjed-Daghi Cu–Au: Jamali et al., 2010; Haftcheshmeh Cu–Mo: Hassanpour et al., 2014], Cu-Fe skarns (Mazraeh: Mollaei et al., 2009) and gold epithermal deposits (Safi Khanlo-Naghdoz: Ghadimzadeh, 2002) (Fig. 1b). Active tectonics of the area and thereafter multiple fractures have provided the conduits for the introduction of hydrothermal fluids derived from intrusive phases into structurally favorable volcanic country rocks and the development of extensive hydrothermal alteration zones associated with different mineralization.

By studying the parameters governing the distribution pattern of trace and rare earth elements (REEs) elements, the geochemical domain of the altered and unaltered zones can be distinguished in the region. Using geochemical studies of REEs by different researchers has provided comprehensive approach to interpret the processes involved in the formation of hypogene alteration zones associated with various mineralization such as copper-gold porphyry and high sulfidation epithermal deposits (Lewis et al., 1997; Takahashi et al., 2004; Parsapoor et al., 2009). These findings show that, contrary to the old hypotheses about the immobility of REEs during alteration and weathering processes, under specific conditions such as low pH, high water/ rock ratio and the abundancy of complexing ligands (i.e. F^-, Cl^-, $CO3^{-2}$, $SO4^{-2}$ and $PO4^{-3}$) they could be mobilized (Michard, 1989). The pH and temperature of fluids can be considered as the most effective controlling factors in mobility of REEs in hydrothermal system. In this research, we have attempted to study trends of development and evolution of altered zones, mineralogical changes, geochemical factors governing the mobility and behavior of REEs, physico-chemical conditions of formation, and reasons for occurrence and changes of Ce and Eu anomalies through the progress of alteration processes.

* Corresponding author. E-mail: Kl_siahcheshm@tabrizu.ac.ir

2 Geological Settings

The Chol-qeshlaghi altered area is located ~15 km east of Ahar ore-field, which is a part of the Qaradagh metallogenic district that is bounded by the great Caucasus Paleo-Tethys suture at the NE and by the Zagros Neo-Tethys suture in the SW (after Dercourt et al., 1986; Aghazadeh et al., 2010). The Qaradagh altered - metallogenic district is situated in the west of the E-W trending Cenozoic Alborz-Azarbaijan magmatic belt (Fig. 1a), near the junction with the Cenozoic NW-trending Urumieh-Dokhtar magmatic belt (Nabavi, 1976; Aghanabati, 2004). According to Moayyed (2001), Tertiary magmatism of the Urumieh-Dokhtar and Western Alborz-Azerbaijan zones are not related to the active subduction of the Neo-Tethys Ocean and can be considered post-collisional magmatic arcs.

Main intrusive bodies in Qaradagh metallogenic belt occurred in Oligocene episode varying in composition of alkali granite, granite through monzonite, granodiorite to diorite and gabbro. They may be assigned to two broad categories (Aghazadeh et al., 2010): (1) calc-alkaline to shoshonitic large plutonic bodies (batholites) with extremely varied composition, medium to coarse grained texture, formed at 3 to 4 km depth and poorly mineralized (e.g. Sheivar Dagh, Khankandi, Youseflu and Kaleibar); (2) porphyritic sub-volcanic bodies with calc-alkaline to alkaline affinities are spatially and temporally associated with NW-SE trending structures, formed at 1–2 km depth, commonly containing remarkable mineralization (e.g. Sungun, Mivehrud, Masjed Daghi and Haftcheshmeh

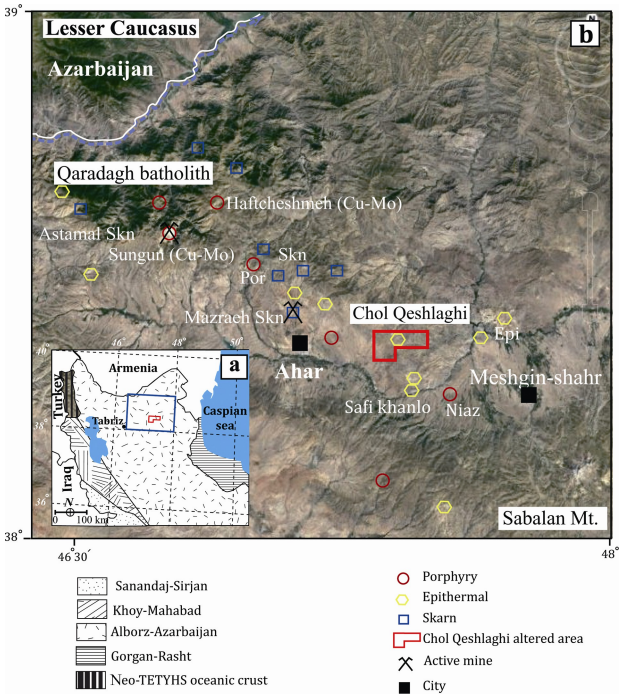

Fig. 1. (a) Sketch map of main tectono- sedimentary zones of NW Iran (modified after Nabavi 1976 and Aghanabati 2004); (b) Landsat google earth image showing and the location of Chol-qeshlaghi altered area within the Qaradagh metallogenic district and distribution of different types of known hydrothermal deposits as well.

deposits). The magmatic activities of the upper Eocene-Oligocene are one of the most interesting and significant geological aspects and are responsible for mineralizing the porphyritic copper, contact metasomatism, and dependent alteration in NW of Iran. This region is underlain by Upper Cretaceous age flysch type rocks and submarine volcanic rocks. The flysch rocks comprise folded micritic limestone, sandstone, shale and mudstone. Upper Cretaceous rocks are unconformably overlain by Mid-Upper Eocene volcano-sedimentary rocks (Mehrpartou, 1999).

The volcanic activities of this area has intermittently continued at least from Eocene to Quaternary, so that are mainly as lava and pyroclastic rocks with a chiefly composition of andesite, trachy-andesite, pyroxene andesite, basalt, andesitic-basalt as well as intensive silicic acidic tuffs, and rhyodacitic tuffs (Fig. 2).

The Khankandi pluton of upper Oligocene age, represents a large regionally exposed NNW-trending batholith close to the Chol-qeshlaghi area. It is a semi elongated ellipsoidal body of 15–20 km length furnished as several magmatic phases of gabbro, monzonite and granodiorite associations (Aghazadeh et al., 2010). in the northern and eastern parts, especially north of the Ahar Chay valley, monzonite and granodiorite are outcropped in the largest area. The monzonites are coarse-grained, mesocratic rocks but porphyritic textures are mainly developed along the marginal parts, close to the contacts with the volcanic country rocks. The granodiorite is characterized by alkali feldspar phenocrysts (1–4 cm length) are set in a medium to coarse-grained matrix composed of plagioclase, quartz, biotite ± amphibole. The boundaries between granodiorites and monzonites are sharp. Some monzonitic to monzo-syenitic dikes crosscut the granodiorites. Fine-grained, rounded mafic microgranular enclaves (5–30 cm length) occur rarely as inclusions in the granodiorites. The Khankandi stock and related similar composition dikes had intruded into the Eocene volcanic rocks during late Oligocene. These dikes have been injected after the end of the alteration and ore-formation in the study area and therefore are classified as post-mineralization dikes. Based on field and petrographic studies, Chol-qeshlaghi alteration is thought to be closely related to the multiple-stage intrusion of Khankandi granodiorite and associated hydrothermal fluids.

3 Sampling and Analytical Methods

A total of 77 samples representing the less altered and altered andesitic rocks were collected from the surface exposures of these rocks and from diamond-drill cores. The 26 samples from of overprinted silicic-argillic, argillic -phyllic, propylitic as well as unaltered andesite and granodiorite were petrographically studied on polished thin sections using transmitted and reflected light. For the identification of mineral phases, 14 samples showing distinct mesoscopic deference in alteration intensity were chosen for X-ray diffraction (XRD) analysis (Table 1) performed using a Bruker D8 Advance Diffractometer with a Cu-anode. Rare earth elements were determined by inductively coupled plasma mass spectrometry (ICP-MS)

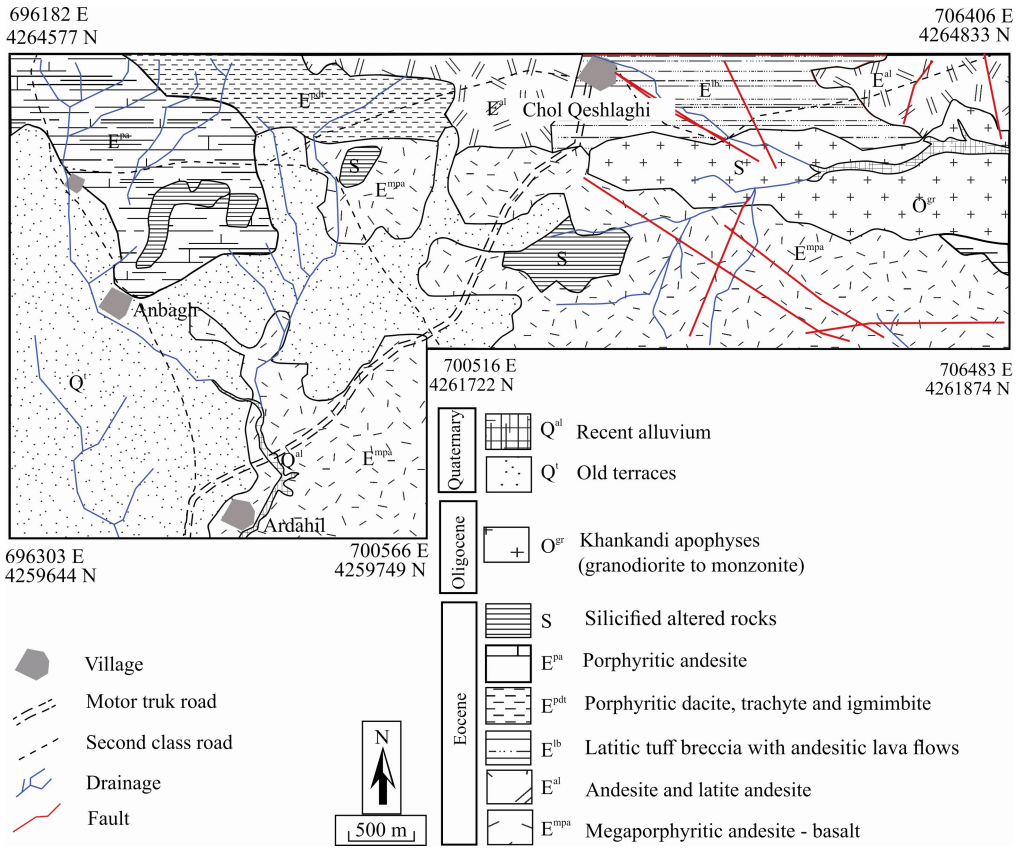

Fig. 2. Geological sketch map of Chol-qeshlaghi prospect area.

Table 1 The results of XRD analyses for the samples from different alteration zones in the Chol-qeshlaghi area

Sample no.	Alteration	Major phases	Accessory phases
Ch-S-3	Silicic	Quartz	Calcite, rutile, chlorite, muscovite
Ch-S-5	Silicic	Quartz	Pyrite, gypsum, muscovite, illite
Ch-S-6	Silicic	Quartz	Alkali feldspar, illite, calcite
Ch-A-6	Argillic	Kaolinite, quartz	Alunite, gypsum, muscovite, chlorite
Ch-A-7	Argillic	Kaolinite, illite	Quartz, Albite, Chlorite, goethite, muscovite
Ch-A-18	Argillic	Kaolinite, montmorillonite	Smectite, alunite, quartz, albite, illite
Ch-A-25	Argillic	Quartz, kaolinite	Illite, muscovite, hematite, chlorite
Ch-P-4	Phyllic	Quartz, muscovite	Kaolinite, jarosite, alunite, anatase, apatite, illite
Ch-P-5	Phyllic	Chlorite, muscovite	Pyrite, albite, kaolinite, illite, alunite,
Ch-P-7	Phyllic	Quartz	Pyrite, chlorite
Ch-PR-1	Propylitic	Epidote, Chlorite	Albite, calcite, hematite
Ch-PR-5	Propylitic	Chlorite, epidote	Quartz, calcite, dolomite
Ch-PR-14	Propylitic	Epidote	Chlorite, plagioclase, calcite
Ch-PR-25	Propylitic	Epidote	Chlorite, calcite, hematite, quartz

method in the ALS-Chemex laboratories, Canada. The detection limits for the analyses were between 0.002 to 0.04 wt% for major elements, 0.1 to 20 ppm for trace elements, and 0.01 to 0.3 ppm for REEs.

In this research, the method of Van Der Weijden and Van Der Weijden (1995) has been applied to calculate mass loss and/or gain, in order to find out the effective factors in the distribution of REEs during the development of different alteration zones.

4 Alteration and Mineralization

Hydrothermal alteration is hosted mainly by latitic tuff, porphyritic andesite, and hydrothermal breccia and comprises siliceous strip veins (0.5 to 10 m width) with outward zonation of phyllic, argillic and restricted propylitic alteration (Figs. 3, 4). The endogenic feldspar destructive alteration in the form of quartz, sericite, chlorite ± clay minerals (Figs. 5 a, b, c) overprinted on the early formed hydrothermal alteration and host rock mineral assemblage as well. This is referred to graduate decreasing in temperature and a $(K^+)/a(H^+)$ ratio of the hydrothermal fluids (Hemley and Hunt, 1992), which produced hydrous silicate phases in the surface oxidized outcrops. Iron oxide products envelope the quartz –sulfide veinlets and/or breccia zones and is characterized by yellowish/brownish or reddish colors (Fig. 4d, e). The widespread occurrence of hydrothermal breccia affected by silicic and argillic alteration (Fig. 4e, f) supports dominant hydrostatic pressure of hydrothermal fluids. The

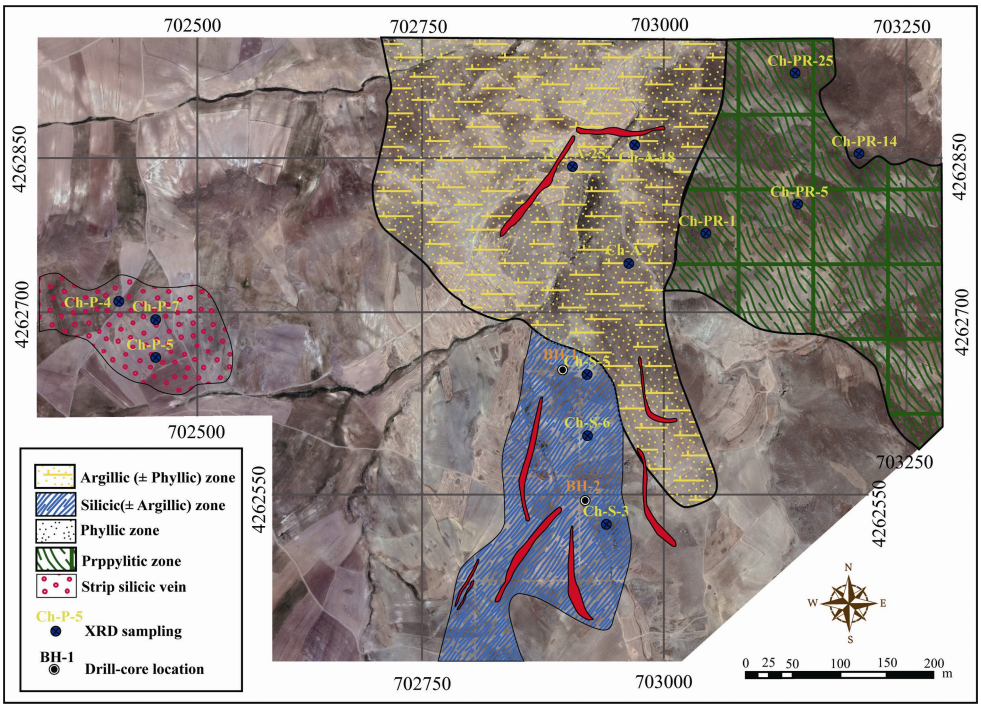

Fig. 3. Alteration zones in Chol-qeshlaghi area and location of the studied samples.

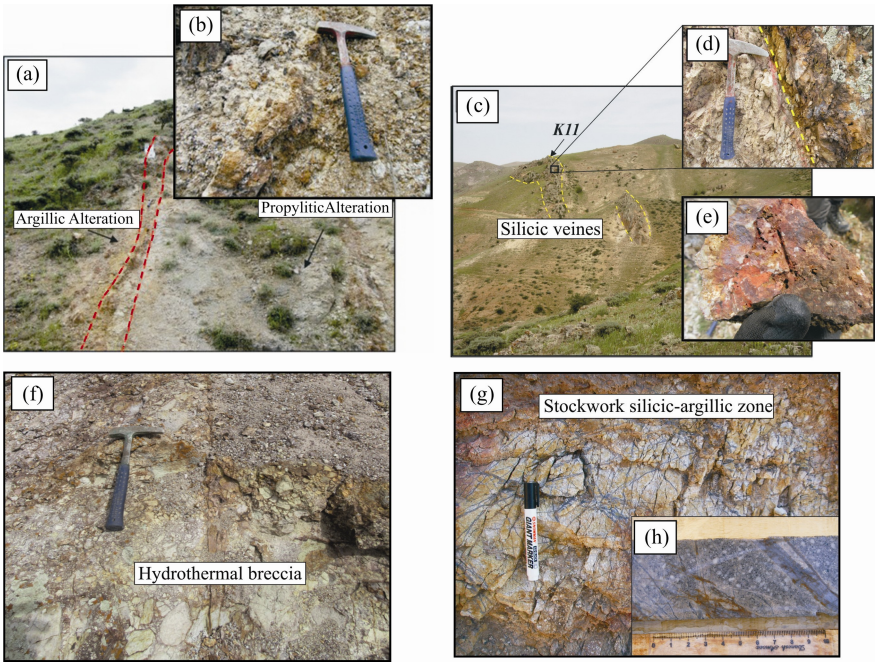

Fig. 4. Outcrops of different alteration zones.
(a, b, c) An exposure of strip /massive silicified zone containing quartz-sulfide veins with outward propylitic and argillic alteration; (d, e) ailicified Iron oxide products envelope quartz –sulfide veinlets and/or shear zones within argillic alteration zone; (f) hydrothermal breccia affected by silicic and argillic alteration; (g, h) stockwork silicic mineralized zone at surface outcrops also diamond drill cores as well.

stockwork silicic altered zone is widely observed at surface outcrops as well as in the selected diamond drill cores (Fig. 4g, h). The advanced argillic in the outcrop comprises quartz+ pyrophyllite+ alunite assemblage, however, it has not a regular coherence. Alunite formed under extremely acidic conditions and/or high activity of the sulfate ion, so the abundance of alunite indicates high activity of H_2S in the reduced volcanic rocks (Zimbelman et al., 2005). Thus, it is anticipated that fluids involved in the formation of alunite alteration zones is causing considerable sulfide mineralization in depth.

Sulfides and sulfosalts mineralization occurs mainly in the silicic cores and the phyllic altered rocks in the form of massive replacement, fractures-filling veinlets, patches

and dissemination. Pyrite, goethite martite and rare covellite are the main constituent of surface mineralization whereas pyrite, chalcopyrite, tennantite and galena are the principle minerals in sub-surface epithermal ore mineralization (Fig. 5d–h). Iron hydroxides (e.g. hematite, goethite) are common late minerals filling in the fractures and coating on the surfaces of mineralized zones. Their occurrences reflect the oxidation of primary sulfides and sulfosalts.

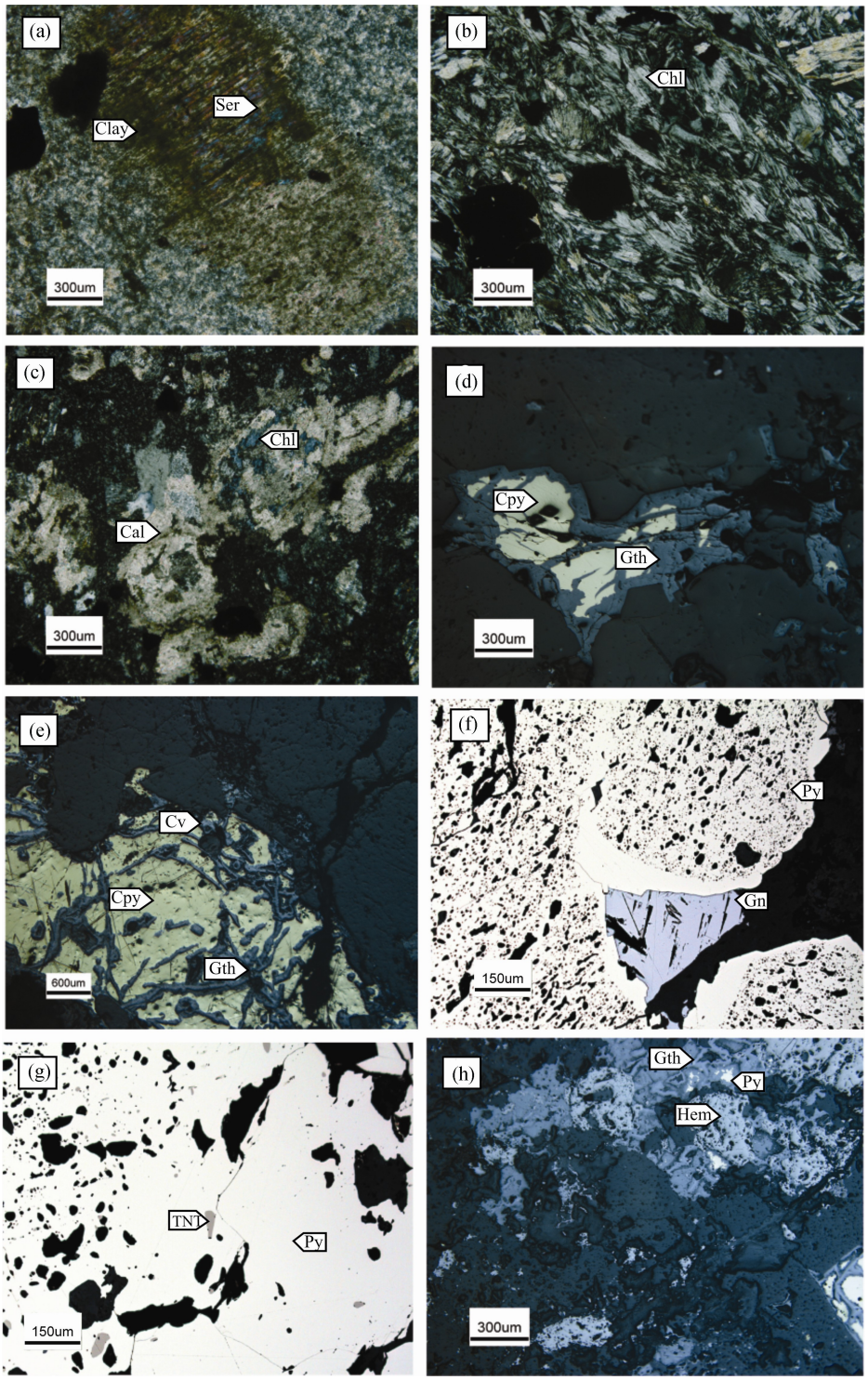

Fig. 5. Photomicrographs of alteration zones and reflected light microscopy.

(a) Alteration offerromagnesian minerals to sericite-paragonite and kaolinite (XPL) in argillic overprinted on phllic zone; (b) fine-grained flakes of chlorite in propylitic zone; (c) formation of calcite and chlorite as replacement products of ferromagnesian minerals (XPL); (d) replacement of chalcopyrite by goethite; (e) slightly corroded along chalcopyrite cracks replaced by goethite and covellite; (f) Galena with triangular cleavage pits associated with pyrite in quartz vein; (g) tennantite after chalcopyrite; (h) alteration of pyrite to goethite and martite after magnetite. Abbreviations for minerals are from Whitney and Evans (2010).

5 Petrography

The mineralogical (Table 1) and paragenetic study has revealed that silicic alteration (quartz, hematite, gypsum, muscovite), phyllic alteration (quartz, pyrite, muscovite, chlorite, and hematite), argillic alteration (kaolinite, quartz, illite, smectite, alunite, muscovite, jarosite, and goethite), and propylitic alteration (quartz, chlorite, calcite, epidote and albite) are major altered zones genetically related to hypogene hydrothermal fluids originated by the intrusion of the Khankandi granodiorite stock into andesite host rocks.

Silicic alteration: Two generations of quartz were identified: the former consists of anastomosing fine - grained patches, chiefly after the silicic alteration of feldspars; the late one typically contains medium- to coarse-grained quartz ± calcite, pyrite, minor chalcopyrite accompanying with sericite ±chlorite selvages and generally cross-cut and offset the argillic mineral assemblages.

Phyllic alteration: This alteration occurred as selective and/or pervasive replacement. In selective alteration, plagioclase is altered to sericite, and biotite and hornblende to chlorite, but pervasive alteration referred as relatively complete breakdown and replacement of all preexisting mineral phases. It is typically overprinted breccia stockwork zones and comprise of quartz-sulfide vein/ veinlets.

Argillic alteration: The late argillic alteration is characterized by nearly complete destruction and replacement of pre-existing mafic minerals (e.g., hornblende, biotite) and feldspars by fine to medium-grained white micas (i.e., muscovite, paragonite), clay minerals (kaolinite, illite-sericite, montmorillonite), quartz, and iron hydroxide (Fig. 4a).

Propylitic alteration: The mineral assemblages within the propylitic alteration zone are typically characterized by replacement of mafic silicate phenocrysts and groundmass by chlorite (Fig. 4b) and local epidote or calcite. Replacement of plagioclase by calcite is a common feature of this zone (Fig. 4c).

6 Mass Changes and Behavior of REEs in the Altered Zones

Mass change calculation by showing enrichment and depletion patterns can be used as a proxy for degree of alteration, and gives an indication of increased proximity to ore. There are two approaches for the calculation of mass changes during alteration processes: (1) iso-volumetric (e.g. Brimhall and Dietrich, 1987; Brimhall et al., 1991) and (2) employing immobile elements (e.g. Nesbitt, 1979; MacLean, 1990; MacLean and Barrett, 1993; Van der Weijden and Van der Weijden, 1995). As a rule, elements such as Al, Zr, and Ti that are not influenced by the alteration processes defined as immobile during hydrothermal processes (Erkoyun and Kadir, 2011; Kadir et al., 2014). In the present study, mass change calculations of REEs and their behavior during different alteration zones were assessed by administering the immobile element equation from Van Der Weijden and Van Der Weijden (1995):

$$\%\text{Change} = F_{(Ti+Zr)} \times [(C^a/°C) - 1] \times 100$$

where $C^a/°C$ is the ratio of the element concentration in the altered and least-altered rock(s). F (Ti + Zr) is used to correct for loss of mass during alteration. The values for $C^a/°C$ of all REEs are multiplied by the same $F_{(Ti+Zr)}$ factor.

Because of relatively wide variation range of immobile elements such as Al, Ti, Hf, Nb, and Zr, in some hydrothermal systems, the changes from −20 to +20 assumed as uncertain range and only the mass changes beyond considered as gains and losses of elements during alteration processes. In these calculations, the negative or positive values represent the mass loss or gain during alteration, respectively. The zero and near-zero values represent the immobility of a given element. The calculation will be emphasized on the four major alteration zones, i.e. silicic, phyllic, argillic and propylitic which occur predominantly in andesite rocks. The results of these calculations are graphically delineated in the form of diagrams (Fig. 6).

6.1 Silicic alteration

The results from the mass changes delineate that in all silicic samples, LREEs and HREEs have been depleted with similar intensity (Figs. 6a and 7a). According to Wood (1990) low temperature (< 350°C), low pH, high oxidation, and abundant sulfur are predominant parameters causing the formation of silicic alteration, and SO_4^{-2} is the major complexing ligand in this zone. When compared SREE to least altered rocks (average 184.3 ppm), the silicic samples indicate considerable decrease in REEs content (average 60.3 ppm). According to Fulignati et al. (1999), this depletion could be attributed to very low pH condition (pH < 2), acidic aggressive fluids, and decomposition of primary minerals. General decrease of REEs in Chol-qeshlaghi silicic zone in comparison with the least altered andesite suggests that it was formed by low-temperature, low pH conditions, and high activity of SO_4^{-2}. Taking into account mineralogy of silicic alteration assemblage, the mass increase of some LREEs in one sample can be referred to preferential adsorption of LREEs by some rutile mineral. It appears that high W/R ratio condition during development of silicic alteration as well as the absent of special minerals that can accommodate LREEs in their structures, provide required conditions for overall depletion of REEs.

6.2 Phyllic alteration

In general, the absolute REE concentration in the phyllic rocks tends to slightly increase. Assuming that increasing of pH causes the REEs deposition in the alteration system, therefore, it could be refereed to abundant faults and fractures in this region that provided a possibility for secondary boiling and then releasing of acidic gasses from hydrothermal fluids, resulting in re-deposit and fix REEs (Figs. 6b and 7b). Enrichment of HREEs in this zone can also be ascribed to easy adsorption onto secondary minerals (Fulignati et al., 1999). Abundance of sericite as well iron oxide due to alteration of pyrite has played a major role in this issue. Moderate to strong positive correlation between Fe and the

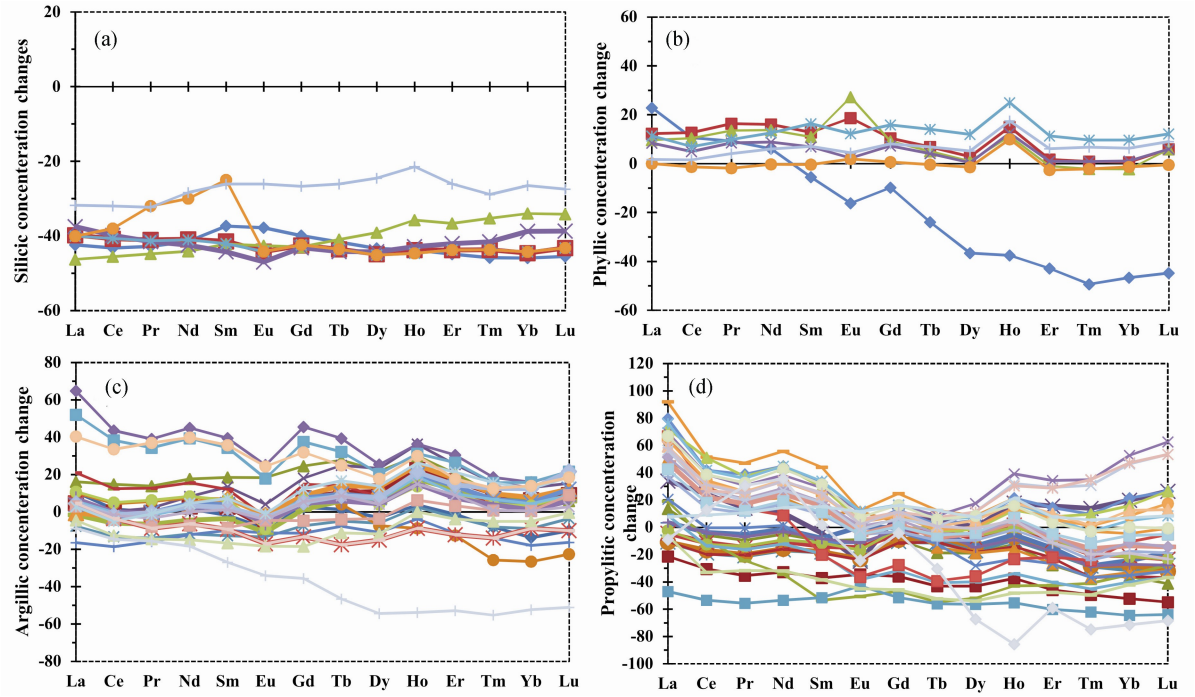

Fig 6. Plots of REEs mass changes in the altered samples relative to their assumed un-altered parent rock (andesite), using F (Ti + Zr) to correct for loss of mass during alteration.

(a) In the sillicic zone (N=7); (b) in the phyllic zone (N=8); (c) in the argillic zone (N=26); (d) in the propylitic zone (N=37).

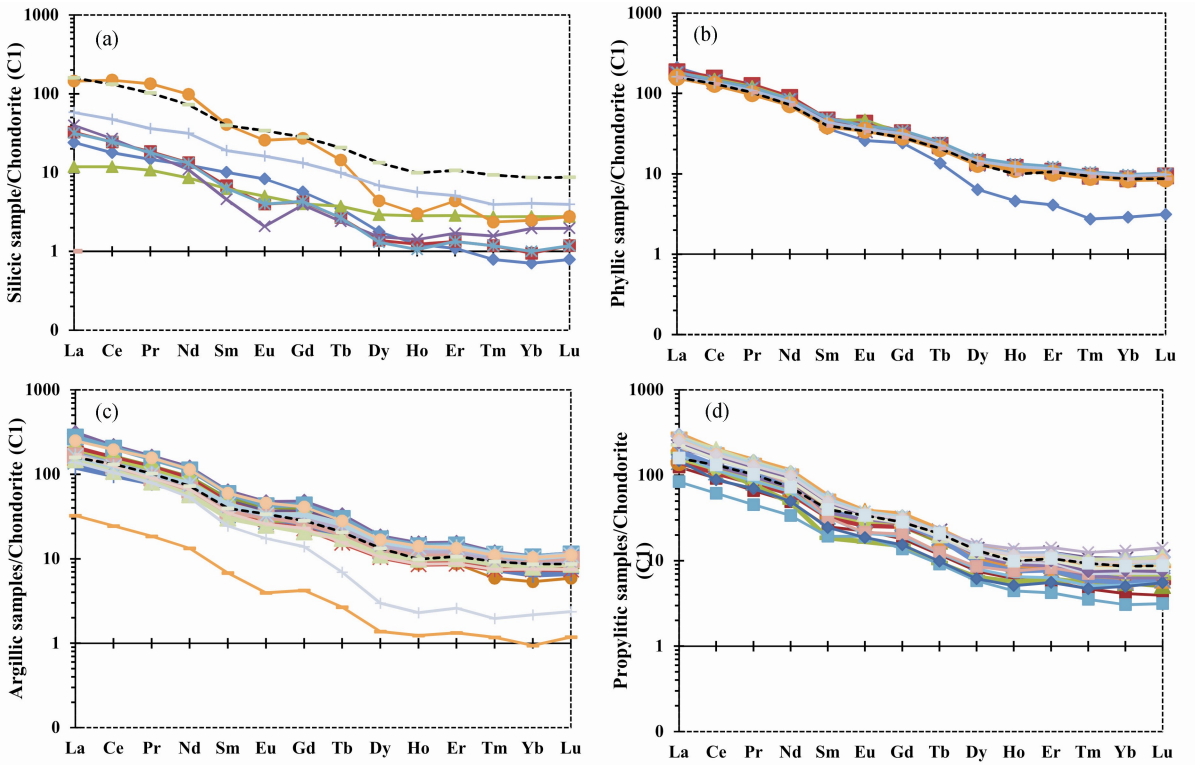

Fig. 7. Distribution pattern of REEs normalized to chondrite (Taylor and McLennan, 1985) in samples taken from.

(a) sillicic; (b) phyllic; (c) argillic; (d) propylitic alteration zones. The dotted line belongs to parent andesitic rock.

total REEs (0.63 to 0.98) demonstrate this fact (Table 3).

6.3 Argillic alteration

The pattern of REEs normalized to the primary andesitic rocks indicate that rare earth elements show individual behaviors during development of this alteration, considering their distribution influenced by both leaching and fixation agents. The changes in acidity of fluids

responsible for argillic alteration, and presence of clay minerals that has the ability to absorb these elements, can be considered as the most outstanding controlling factor for the distribution, mobility and enrichment of rare earth elements in the argillic zone. At low pH conditions, clay minerals have low absorption capacity for these elements (Michard, 1989). In the samples taken from outer parts of zone, LREEs depletion with respect to less altered rocks are probably due to leaching and low cation exchange capacity of clay minerals (Fig. 6c). In fact, hypogene fluids, in addition to having low pH, have caused the depletion of rare earth elements from the system due to the high W/R ratio and the abundance of complexing ligands. The enrichment of rare earth elements in samples that are far from the position of the faults shows that the pH of the altering solutions has increased, which has led to the stabilization and enrichment of rare earth elements in the system.

Calculating the Pearson correlation coefficients between rare earth elements with selective major and trace elements can clarify some other interesting geochemical features of the argillic alteration zone. The positive and moderate correlations between Al and the total REEs (r = 0.51 to 0.65) points the fact that clay minerals have an important controlling role in the distribution of rarest earth elements in this zone. Strong positive correlations between the total REEs with Fe (0.58 to 0.92) and Mn (0.53 to 0.81) suggests that Fe and Mn oxides and hydroxides play an important role in the concentration and stabilization of REEs. In other words, the distribution pattern of REEs in this zone seems to be controlled by the deposition of iron and manganese. The positive and moderate correlation coefficients between P and the total REEs (r = 0.60 to 0.66) can be indicative of controlling the distribution some part of REEs by secondary phosphate minerals (Table 4). Similarly, the positive and strong correlation between Y and the total lanthanides (0.72 to 0.90) indicates the presence of xenotime (YPO4) mineral in this zone. Moreover, the positive and average correlation between Ti and the total REEs (0.55 to 0.68) suggests that Ti-bearing mineral phases play an effective role at REEs concentrations in this zone (Lopez et al., 2005). Moderate and positive correlation between Th and Ce is a reason for the probable presence of monazite mineral. In general, difference in the rate of resistance of the early minerals to the alteration and/or heterogeneity of precursor rock can be considered as only logical reason for creating irregularity at the REEs distribution trends in the studied

Table 2 REE distribution (ppm) in the different alteration zones from Chol-qeshlaghi area compared with less altered andesitic rocks

	Sample no	La	Ce	Pr	Nd	Sm	Eu	Gd	Tb	Dy	Ho	Er	Tm	Yb	Lu	ΣREE	*Ce/Ce	*Eu/Eu
Fresh andesite	An-F-1	34.90	72.90	8.98	31.50	5.80	1.74	5.24	0.72	3.17	0.62	1.65	0.22	1.41	0.21	34.90	0.99	0.96
	An-F-2	45.30	94.60	11.10	36.90	6.21	1.83	6.11	0.80	3.52	0.68	1.88	0.26	1.64	0.25	45.30	1.00	0.91
	An-F-3	47.40	99.30	11.50	37.80	6.39	1.81	6.14	0.81	3.51	0.68	1.90	0.27	1.67	0.26	47.40	1.01	0.88
	An-F-4	30.70	63.50	7.96	29.00	5.36	1.79	5.17	0.68	3.00	0.57	1.53	0.21	1.27	0.19	30.70	0.97	1.04
	An-F-5	38.50	89.30	10.45	37.00	6.69	2.33	6.36	0.84	3.60	0.60	1.81	0.23	1.41	0.21	38.50	1.07	1.09
	An-F-6	34.20	75.90	9.30	32.90	5.96	2.28	5.62	0.74	3.23	0.06	1.60	0.21	1.25	0.18	34.20	1.02	1.20
	An-F-7	32.20	69.90	8.76	32.30	6.19	1.98	6.09	0.83	3.70	0.71	1.92	0.26	1.62	0.25	32.20	1.00	0.99
Silicic zone	An-S-1	5.70	10.95	1.40	5.80	1.54	0.48	1.17	0.13	0.45	0.07	0.18	0.02	0.12	0.02	5.70	0.92	1.09
	An-S-2	7.70	14.95	1.75	6.20	1.04	0.23	0.87	0.10	0.35	0.07	0.22	0.03	0.16	0.03	7.70	0.96	0.74
	An-S-3	2.80	7.24	1.02	4.00	0.95	0.29	0.82	0.14	0.74	0.16	0.47	0.07	0.47	0.07	2.80	1.05	1.00
	An-S-4	9.40	16.45	1.65	5.10	0.70	0.12	0.80	0.09	0.39	0.08	0.28	0.04	0.33	0.05	9.40	0.94	0.49
	An-S-5	7.50	15.05	1.70	6.10	0.97	0.23	0.89	0.10	0.33	0.06	0.22	0.03	0.17	0.03	7.50	0.99	0.76
	An-S-6	34.20	91.10	12.70	46.00	6.20	1.49	5.57	0.54	1.11	0.17	0.72	0.06	0.42	0.07	34.20	1.07	0.78
	An-S-7	13.70	29.10	3.44	14.70	2.91	0.94	2.71	0.37	1.73	0.32	0.84	0.10	0.69	0.10	13.70	1.01	1.02
Argillic alteration zone	An-A-1	43.30	82.60	9.72	34.70	5.93	1.72	6.03	0.79	3.24	0.59	1.72	0.21	1.18	0.19	43.30	0.95	0.88
	An-A-2	40.10	80.50	9.67	35.40	6.34	1.74	6.43	0.89	3.92	0.74	2.17	0.27	1.60	0.25	40.10	0.97	0.83
	An-A-3	46.30	97.90	11.65	42.50	7.69	2.48	7.86	1.08	4.45	0.80	2.27	0.27	1.59	0.24	46.30	1.01	0.98
	An-A-4	40.40	81.10	10.00	37.90	7.25	2.08	7.32	1.05	4.52	0.85	2.39	0.29	1.74	0.27	40.40	0.96	0.87
	An-A-5	33.50	65.50	7.79	28.20	4.98	1.59	5.20	0.72	3.10	0.58	1.68	0.21	1.28	0.21	33.50	0.96	0.96
	An-A-6	43.10	85.80	10.50	37.60	6.69	1.93	6.35	0.82	3.03	0.49	1.44	0.15	0.91	0.15	43.10	0.96	0.91
	An-A-7	28.80	59.30	7.51	28.00	5.23	1.65	4.88	0.69	2.86	0.53	1.47	0.19	1.09	0.17	28.80	0.97	1.00
	An-A-8	48.90	95.10	11.50	41.50	7.13	1.89	7.05	0.93	3.78	0.70	2.07	0.25	1.52	0.24	48.90	0.95	0.81
	An-A-9	36.80	73.80	8.81	31.80	5.78	1.66	5.93	0.84	3.65	0.70	2.05	0.26	1.52	0.24	36.80	0.97	0.87
	An-A-10	72.40	131	15.15	55.70	9.52	2.67	9.60	1.21	4.62	0.85	2.52	0.30	1.80	0.29	72.40	0.92	0.85
	An-A-11	65.60	125	14.50	53.00	9.08	2.47	8.94	1.13	4.38	0.81	2.42	0.29	1.80	0.29	65.60	0.95	0.84
	An-A-12	37.30	77.80	9.55	36.10	6.71	1.92	6.55	0.93	4.04	0.76	2.20	0.27	1.63	0.26	37.30	0.99	0.89
	An-A-13	39.80	77.60	9.68	36.10	6.43	1.77	6.43	0.88	3.76	0.72	2.10	0.26	1.57	0.26	39.80	0.94	0.84
	An-A-14	40.10	76.60	8.50	30.90	5.28	1.49	4.72	0.58	2.66	0.49	1.45	0.19	1.28	0.19	40.10	0.97	0.91
	An-A-15	43.40	86.60	10.60	38.00	6.63	1.71	6.37	0.87	3.58	0.67	1.99	0.25	1.54	0.25	43.40	0.96	0.80
	An-A-16	41.40	80.60	9.61	35.10	6.32	1.80	6.21	0.84	3.60	0.68	1.94	0.25	1.49	0.24	41.40	0.95	0.88
	An-A-17	40.70	80.50	9.48	35.10	6.35	1.86	6.40	0.87	3.70	0.71	2.00	0.26	1.56	0.25	40.70	0.97	0.89
	An-A-18	7.70	14.95	1.75	6.20	1.04	0.23	0.87	0.10	0.35	0.07	0.22	0.03	0.16	0.03	7.70	0.96	0.74
	An-A-19	40.00	78.80	9.68	35.50	6.30	1.88	6.25	0.87	3.76	0.73	2.12	0.28	1.73	0.29	40.00	0.95	0.92
	An-A-20	39.20	76.10	8.64	30.40	5.35	1.84	5.43	0.73	3.22	0.61	1.84	0.24	1.48	0.25	39.20	0.97	1.04
	An-A-21	35.20	66.20	7.71	26.70	4.63	1.45	4.28	0.65	2.82	0.56	1.66	0.22	1.36	0.22	35.20	0.94	1.00
	An-A-22	39.40	78.50	9.27	33.90	6.19	1.85	6.28	0.87	3.59	0.68	1.98	0.24	1.48	0.23	39.40	0.97	0.91
	An-A-23	39.10	75.00	9.58	36.10	6.72	1.94	6.85	0.96	4.06	0.77	2.29	0.29	1.73	0.28	39.10	0.92	0.87
	An-A-24	59.30	119.50	14.85	53.20	9.19	2.65	8.47	1.05	4.25	0.80	2.20	0.28	1.76	0.28	59.30	0.96	0.92
	An-A-25	32.90	63.90	7.56	25.00	3.74	1.01	2.86	0.26	0.76	0.13	0.43	0.05	0.37	0.06	32.90	0.96	0.94
	An-A-26	40.10	76.60	8.50	30.90	5.28	1.49	4.72	0.58	2.66	0.49	1.45	0.19	1.28	0.19	40.10	0.97	0.91

Table 2 Continued

	Sample no	La	Ce	Pr	Nd	Sm	Eu	Gd	Tb	Dy	Ho	Er	Tm	Yb	Lu	ΣREE	*Ce/Ce	*Eu/Eu
Phyllic zone	An-PH-1	49.90	93.00	11.00	36.90	5.61	1.51	5.00	0.51	1.62	0.26	0.68	0.07	0.49	0.08	49.90	0.93	0.87
	An-PH-2	44.20	95.40	12.00	41.70	7.20	2.49	6.68	0.85	3.53	0.68	1.80	0.24	1.48	0.24	44.20	1.00	1.10
	An-PH-3	42.80	92.80	11.60	40.60	7.04	2.73	6.58	0.83	3.44	0.65	1.73	0.23	1.42	0.24	42.80	1.00	1.23
	An-PH-4	42.10	86.50	10.90	38.20	6.68	2.03	6.42	0.82	3.41	0.66	1.78	0.24	1.49	0.24	42.10	0.97	0.95
	An-PH-5	43.70	88.80	11.10	40.00	7.51	2.31	7.14	0.93	3.97	0.76	2.04	0.27	1.67	0.26	43.70	0.96	0.96
	An-PH-6	37.60	79.30	9.46	33.80	6.05	2.02	5.87	0.77	3.32	0.64	1.69	0.23	1.44	0.22	37.60	1.00	1.04
	An-PH-7	38.50	82.60	10.30	36.80	6.70	2.09	6.49	0.85	3.64	0.70	1.91	0.26	1.60	0.25	38.50	1.00	0.97
	An-PH-8	2.80	7.24	1.02	4.00	0.95	0.29	0.82	0.14	0.74	0.16	0.47	0.07	0.47	0.07	2.80	1.05	1.00
Propylitic alteration zone	An-PR-1	6.40	12.25	1.34	4.70	0.82	0.26	0.90	0.11	0.42	0.08	0.23	0.03	0.20	0.03	6.40	0.97	0.93
	An-PR-2	29.60	56.10	6.28	22.80	3.83	1.29	3.73	0.44	1.93	0.35	0.95	0.12	0.70	0.10	29.60	0.96	1.04
	An-PR-3	42.70	76.10	8.80	32.20	5.48	1.79	5.27	0.63	2.75	0.49	1.27	0.15	0.94	0.13	42.70	0.91	1.02
	An-PR-4	50.40	100.50	11.10	37.50	5.82	1.48	6.38	0.82	3.40	0.66	2.03	0.27	1.76	0.28	50.40	1.00	0.74
	An-PR-5	33.60	65.70	7.71	28.30	4.99	1.51	5.22	0.69	2.81	0.51	1.43	0.17	1.01	0.16	33.60	0.96	0.90
	An-PR-6	33.50	67.10	7.78	28.60	5.00	1.51	5.29	0.72	2.90	0.52	1.47	0.17	1.06	0.15	33.50	0.98	0.90
	An-PR-7	38.90	77.80	9.21	33.40	5.60	1.97	5.81	0.75	2.92	0.53	1.49	0.17	1.11	0.18	38.90	0.97	1.06
	An-PR-8	33.70	64.80	7.75	28.50	4.93	1.50	5.16	0.69	2.77	0.48	1.36	0.15	0.94	0.14	33.70	0.95	0.91
	An-PR-9	44.80	73.00	7.36	22.30	2.84	0.97	3.09	0.35	1.63	0.32	1.01	0.14	0.96	0.16	44.80	0.90	1.00
	An-PR-10	8.00	12.25	1.51	5.80	1.21	0.38	1.05	0.12	0.46	0.07	0.19	0.02	0.14	0.02	8.00	0.81	1.03
	An-PR-11	19.90	37.60	4.31	15.80	2.95	1.12	2.82	0.34	1.48	0.25	0.70	0.09	0.52	0.08	19.90	0.95	1.19
	An-PR-12	56.40	104.50	11.60	41.30	6.66	2.19	6.02	0.66	2.75	0.47	1.29	0.15	0.98	0.15	56.40	0.95	1.06
	An-PR-13	45.40	80.50	9.69	34.40	5.42	1.74	5.61	0.68	2.44	0.43	1.29	0.15	0.95	0.15	45.40	0.90	0.96
	An-PR-14	36.00	71.70	8.29	30.40	5.24	1.67	5.57	0.76	3.12	0.57	1.59	0.19	1.16	0.17	36.00	0.98	0.95
	An-PR-15	36.80	70.70	8.38	30.80	5.39	1.64	5.74	0.78	3.17	0.56	1.61	0.19	1.15	0.17	36.80	0.95	0.90
	An-PR-16	39.00	77.70	9.03	32.90	5.57	1.74	5.72	0.75	2.89	0.51	1.44	0.17	1.07	0.16	39.00	0.98	0.94
	An-PR-17	40.90	69.90	8.13	29.80	4.90	1.21	3.98	0.46	2.04	0.37	1.05	0.13	0.88	0.14	40.90	0.88	0.84
	An-PR-18	72.20	122.50	14.30	52.80	8.77	2.21	7.26	0.87	3.68	0.68	1.87	0.23	1.40	0.22	72.20	0.88	0.85
	An-PR-19	67.60	114.50	13.50	49.10	8.09	2.00	6.57	0.79	3.56	0.68	2.01	0.26	1.78	0.28	67.60	0.88	0.84
	An-PR-20	62.70	105.00	11.05	36.90	4.87	1.25	4.22	0.47	2.18	0.43	1.37	0.18	1.31	0.21	62.70	0.90	0.84
	An-PR-21	64.70	122.00	13.35	49.00	7.89	2.07	6.46	0.75	3.34	0.63	1.89	0.26	1.70	0.28	64.70	0.96	0.89
	An-PR-22	63.70	112.00	12.70	46.90	7.85	2.20	6.76	0.84	3.98	0.78	2.36	0.32	2.24	0.36	63.70	0.91	0.92
	An-PR-23	66.20	114.50	13.20	49.10	8.15	2.20	6.78	0.82	3.64	0.66	1.88	0.23	1.54	0.24	66.20	0.89	0.90
	An-PR-24	61.70	108.50	12.25	45.30	7.51	2.04	6.30	0.76	3.40	0.64	1.86	0.24	1.59	0.26	61.70	0.91	0.91
	An-PR-25	51.60	92.10	10.75	39.80	6.65	1.86	5.65	0.70	3.07	0.55	1.55	0.18	1.21	0.18	51.60	0.91	0.93
	An-PR-26	55.50	98.70	11.40	42.10	7.05	1.86	5.93	0.72	3.23	0.58	1.62	0.20	1.27	0.19	55.50	0.91	0.88
	An-PR-27	35.20	54.20	6.65	23.10	3.75	1.08	3.16	0.37	1.56	0.29	0.92	0.12	0.85	0.14	35.20	0.81	0.96
	An-PR-28	57.00	102.50	11.75	43.60	7.23	1.98	6.14	0.74	3.21	0.59	1.64	0.19	1.30	0.19	57.00	0.92	0.91
	An-PR-29	53.60	95.30	10.90	40.40	6.76	1.86	5.85	0.73	3.25	0.60	1.67	0.21	1.38	0.21	53.60	0.91	0.90
	An-PR-30	59.90	106.50	12.25	45.60	7.53	2.04	6.41	0.78	3.56	0.66	1.93	0.24	1.65	0.25	59.90	0.91	0.90
	An-PR-31	58.90	102.50	11.65	43.10	7.19	1.93	6.20	0.78	3.77	0.74	2.27	0.31	2.15	0.34	58.90	0.90	0.88
	An-PR-32	59.90	102.50	12.15	45.50	7.53	2.08	6.47	0.83	3.77	0.73	2.26	0.32	2.16	0.34	59.90	0.88	0.91
	An-PR-33	62.80	112.00	12.90	48.40	8.00	2.11	6.77	0.82	3.68	0.65	1.82	0.23	1.47	0.22	62.80	0.91	0.88
	An-PR-34	59.50	106.00	12.15	45.30	7.63	2.01	6.49	0.78	3.36	0.59	1.56	0.19	1.19	0.17	59.50	0.91	0.87
	An-PR-35	40.50	88.00	10.75	38.80	7.01	2.19	6.76	0.87	3.64	0.68	1.89	0.25	1.57	0.24	40.50	1.01	0.97
	An-PR-36	7.50	15.05	1.70	6.10	0.97	0.23	0.89	0.10	0.33	0.17	0.22	0.03	0.17	0.03	7.50	0.99	0.76
	An-PR-37	34.20	91.10	12.70	46.00	6.20	1.49	5.57	0.54	1.11	0.08	0.72	0.06	0.42	0.07	34.20	1.07	0.78

samples.

6.4 Propylitic alteration

Figure 6d clearly shows both incremental and decremented trends in the concentration of REEs during the development of propylitic alteration zone, pointing out that the changes in the pH of the fluids responsible for alteration have been one of the most important factors controlling distribution of lanthanides in different amounts (Patino et al., 2003). It appears that the increase in pH of the fluids responsible for alteration has provided favorable conditions for REEs scavenging and fixation by scavengers such as chlorite in this zone. Positive and moderate correlations of Mg with the total REEs (r = 0.55 to 0.78) represent this process. By increasing the pH of the fluids, associated with the relative enrichment of REEs, the preferential absorption of LREEs and HREEs was more severe than MREEs (Figs. 6d and 7d). We infer that stabilization into the neomorph mineral phases and the resistance of REEs-bearing minerals in primary rock against the alteration, were two outstanding factors that played a significant role in comparison to ionic potential at distribution and concentration of REEs during formation and development of propylitic zone.

Table 3 The Pearson's correlation coefficients between the total REE and the selective major and trace elements in phyllic altered samples

	Si	Al	Fe	Ti	Mn	P	Th	Y	Hf	Zr
La	−0.09	0.96	0.97	0.68	0.46	0.92	0.64	0.72	0.10	0.11
Ce	−0.03	0.97	0.98	0.74	0.59	0.94	0.70	0.74	0.13	0.14
Pr	0.01	0.97	0.98	0.78	0.63	0.93	0.73	0.76	0.17	0.17
Nd	−0.03	0.97	0.98	0.78	0.67	0.94	0.72	0.79	0.16	0.16
Sm	−0.11	0.95	0.96	0.79	0.78	0.91	0.69	0.84	0.17	0.16
Eu	−0.08	0.87	0.88	0.87	0.85	0.82	0.77	0.84	0.31	0.30
Gd	−0.23	0.94	0.94	0.78	0.81	0.90	0.67	0.88	0.16	0.15
Tb	−0.31	0.88	0.87	0.77	0.90	0.83	0.64	0.92	0.19	0.18
Dy	−0.33	0.08	0.07	−0.10	0.22	0.31	−0.16	0.96	−0.48	−0.48
Ho	−0.36	0.73	0.72	0.72	0.97	0.68	0.56	0.98	0.23	0.21
Er	−0.37	0.71	0.70	0.70	0.97	0.66	0.55	0.98	0.22	0.20
Tm	−0.37	0.65	0.63	0.68	0.98	0.60	0.52	0.98	0.24	0.21
Yb	−0.32	0.66	0.64	0.67	0.97	0.61	0.51	0.98	0.22	0.20
Lu	−0.32	0.67	0.66	0.73	0.98	0.62	0.59	0.97	0.29	0.27

Table 4 Summary of microthermometric data for Type IV (LV) and Type V (LVS) fluid inclusions in garnets from the magnetite–garnet skarn

	Si	Al	Fe	Ti	Mn	P	Th	Y	Hf	Zr
La	−0.03	0.51	0.58	0.55	0.53	0.66	0.56	0.78	0.48	0.47
Ce	−0.01	0.56	0.62	0.56	0.57	0.61	0.55	0.77	0.45	0.43
Pr	0.01	0.58	0.65	0.61	0.59	0.62	0.48	0.73	0.44	0.42
Nd	−0.04	0.58	0.69	0.63	0.62	0.60	0.45	0.75	0.44	0.42
Sm	−0.09	0.60	0.76	0.67	0.66	0.60	0.40	0.86	0.40	0.38
Eu	−0.07	0.65	0.77	0.62	0.67	0.63	0.39	0.86	0.32	0.30
Gd	−0.20	0.57	0.82	0.68	0.71	0.61	0.35	0.89	0.36	0.35
Tb	−0.30	0.58	0.88	0.68	0.75	0.66	0.28	0.74	0.32	0.31
Dy	−0.32	0.58	0.92	0.65	0.79	0.65	0.28	0.72	0.34	0.32
Ho	−0.35	0.56	0.93	0.65	0.81	0.62	0.26	0.90	0.37	0.35
Er	−0.37	0.55	0.92	0.63	0.81	0.61	0.29	0.89	0.39	0.37
Tm	−0.35	0.53	0.92	0.59	0.80	0.62	0.30	0.88	0.44	0.42
Yb	−0.30	0.54	0.90	0.57	0.79	0.63	0.36	0.89	0.51	0.48
Lu	−0.31	0.52	0.89	0.55	0.79	0.62	0.31	0.90	0.53	0.50

7 Evolution of Eu and Ce Anomalies

In order to make better interpretations and to realize effective factors at REEs distribution in the alteration zones, REEs values were normalized to chondritic composition (Taylor and McLennan, 1985) and Eu and Ce anomalies were calculated using the following equations:

$Eu/Eu^{*} = Eu_N/(Sm_N \cdot Gd_N)^{0.5}$

$Ce/Ce^{*} = 2Ce_N/(La_N \cdot Pr_N)^{0.5}$

Chondrite normalized REEs distribution patterns (Fig. 7) indicate differentiation and enrichment of the LREEs relative to HREEs, occurrence of weak negative Eu anomalies and Ce anomalies near unit during the alteration process in all four zones. Eu and Ce negative anomalies of silicic and argillic zones among the all studies altered units, are more intense than in others. The presence of alunite in argillic zone, that can accommodate and stabilize LREEs in its lattice, can be assumed as a reason for fractionation and enrichment of the LREEs with respect to the HREEs. In the silicic altered samples, LREEs and HREEs are both leached with a similar intensity (except of sample An-S-7). In the propylitic alteration zone, the distribution trend for HREEs is roughly flat. Phyllic altered samples (Fig. 7b) have similar LREEs values, and, while are enriched in HREEs, but they have less differentiated.

Based on Fig. 8, the Eu/Eu^{*} ratios in argillic and propylitic alteration zones is slightly less than least altered samples. Negative anomaly in the argillic zone are related to the high activity of complexing $SO4^{-2}$ ions in argillic acid-sulfate fluids, which are eventually responsible for carrying REEs. The oxidation of endogenic pyrites and subsequent formation of exogenic acidic solutions is another factor that has been shown to weaken clay minerals operations for the Eu adsorption. The occurrence of negative Eu anomalies in the argillic zone seems to be a function of the pH- Eh and temperature of the alteration fluids as well as the oxidation of the endogenic sulfides. $(Eu/Eu^{*}) < 1$ values in the propylitic zone suggests that during the plagioclase alteration and the formation of albite, some Eu, which was substituted Ca in the early calcic plagioclases lattice, has been released as Eu^{2+} and leached by hydrothermal fluids. On the other hand, because the abundance of hydrothermal sulfides in this zone is very slight, Eu has not been allowed to concentrate and remain in the zone. However, in the silica alteration zone, a significant reduction in the amount of Eu/Eu^{*} is a function of the pH and the temperature of the alteration fluids. The acid leaching of elements and presence of scarce hydrothermal sulfides and clay minerals have prompted little absorption of Eu. In the path of the mother rock to the silica alteration zone, the reduction of the Eu anomalies along with Na and Ca depletion indicates the continual alteration of plagioclase as the degree of alteration intensifies. The Eu anomaly in the Phyllic alteration zone is minimal and its values does not change during the alteration processes with respect to the primary rock. It illuminates that the pH of the alteration system has scarcely vary during development and evolution.

The (Ce/Ce^{*}) ratio value in propylitic, argillic, and phyllic zones is hardly smaller than fresh samples and silicic zone, suggested that some Ce has been released and leaved as Ce^{3+} by hydrothermal fluids (Fig. 8). These

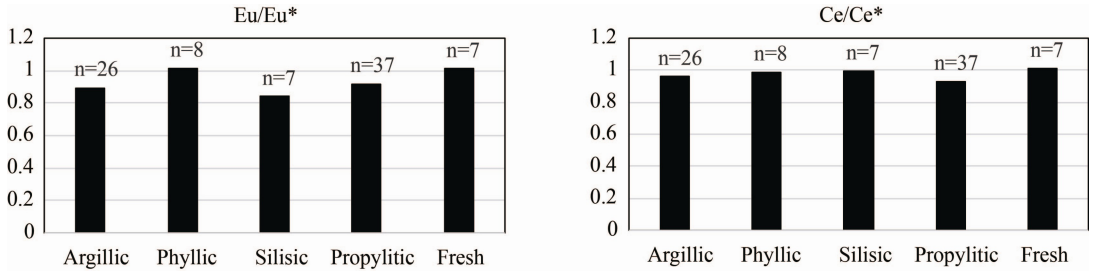

Fig. 8. The display of the column mean values of Eu/Eu* and Ce/Ce* normalized to chondrite (Taylor and McLennan 1985) in different alteration zones.

negative anomalies may be related to the fractionation of the mineral zircon under oxidizing acidic fluid conditions (Fulignati et al., 1999; Karakaya, 2009). The reason for this is to increase the stability of REEs complexing ligands by increasing the temperature (Hass et al., 1995). Minor changes of the Ce anomaly indicate that the oxidation potential condition has not changed much during evolution of alteration system.

8 Conclusions

Based on the results and discussion elaborated above, we draw the following conclusions:

Hydrothermal leaching and stabilization are the main factors controlling the REEs distribution in Chol-qeshlaghi altered system. Obviously, during the formation of the silicic zone, the most LREEs and MREEs have removed from the system identically, affected by the relatively low pH condition and the high activity of SO_4^{-2} in the responsible alteration fluids.

Large quantity of sericite as well as iron oxide, produced by alteration of pyrite, has played an important role in enrichment of HREEs in the phyllic zone. In the argillic and propylitic zones, the REEs have been subjected to both increasing and decreasing mass. The LREEs depletion outward of the argillic zone relative to the less altered rocks is probably due to the low cation exchange capacity of clay minerals in acidic-pH conditions. Positive correlations of REEs with Fe and Mn suggests that Fe and Mn oxides and hydroxides played an important role in the REEs concentrations. Relative LREEs and HREEs enrichment in comparison with MREEs denotes their fixation by neomorph mineral phases as the major scavenger of this elements during the formation and development of the propylitic zone. Sevier loss of Eu mass elucidating the distinctive feature of the silicic zone. Acidic leaching and the low quantity of the hydrothermal sulfides and clay minerals caused the concentration and absorption of released Eu^{2+} to be very small. The negative Eu anomalies in the argillic zone can be attributed to the function of the high activity of complexing sulfate ions, reducing in pH caused by the endogenic pyrite oxidation, and high fO_2 of the hydrothermal system.

Manuscript received Nov. 30, 2018
accepted Feb. 14, 2019
associate EIC: HAO Ziguo
edited by Jeff LISTON and FEI Hongcai

References

Aghanabati, A., 2004. Geology of Iran: Geological Survey of Iran (in Persian).

Aghazadeh, M., Castro, A., Badrzadeh, Z., and Vogt, K., 2011. Post-collisional polycyclic plutonism from the Zagros hinterland: the Shaivar Dagh plutonic complex, Alborz belt, Iran. Geological Magazine Cambridge University Press, 1–29.

Aghazadeh, M., Castro, A., Rashidnejad Omran, N., Emami, M.H., Moinvaziri, H., and Badrzadeh, Z., 2010. The gabbro (shoshonitic)-monzonite-granodiorite association of Khankandi pluton, Alborz Mountains, NW Iran, Journal of Asian Earth Sciences, 38: 199–219.

Brimhall, G.H., Lewis, C.J., Ford, C., Bratt, J., Taylor, G., and Warin, O., 1991. Quantitative geochemical approach to pedogenesis: importance of parent material reduction, volumetric expansion and eolian influx in laterization. Geoderma, 51: 51–91

Brimhall, GH., and Dietrich, WE., 1987. Constitutive mass balance differential feldspar weathering in granites relations between chemical composition, volume, density, porosity, and strain in metasomatic hydrochemical systems: results on weathering and pedrogenesis. Geochim Cosmochim Ac, 51: 567–587.

Calagari, A.A., 2004. Fluid inclusion studies in quartz veinlets in the porphyry copper deposit at Sungun, East-Azarbaidjan, Iran. Journal of Asian Earth Sciences, 23: 179–189.

Dercourt, J., Zonenshain, L.P., Ricou, L.-E., Kazmin, V.G., Le Pichon, X., Knipper, A.L., Grandjacquet, C., Sbortshikov, I.M., Geyssant, J., Lepvrier, C., Pechersky, D.H., Boulin, J., Sibuet, J.-C., Savostin, L.A., Sorokhtin, O., Westphal, M., Bazhenov, M.L., Lauer, J.P., Biju-Duval, B., 1986. Geological evolution of the Tethys belt from the Atlantic to the Pamirs since the Lias, Tectonophysics, 123: 241–315.

Erkoyun, H., and Kadir, S., 2011. Mineralogy, micromorphology, geochemistry and genesis of a hydrothermal kaolinite deposit and altered Miocene host volcanites in the Hallaclar area, Uşak, western Turkey. Clay Mineral, 46: 421–448.

Fulignati, P., Gioncada, A., and Sbrana, A., 1999. Rare earth element (REE) behaviour in the alteration facies of the active magmatichydrothermal system of Vulcano (Aeolian Islands, Italy). Jouranl of Volcanol Geotherm Research, 88: 325–342.

Ghadimzade, H., 2002. Economic Geology and gold exploration in Safi Khanlo-Naghdoz exploration area (south east of Ahar). Msc thesis, Institute of Earth Science, Geological survey, Tehran, Iran 193 (in Persian with English abstract).

Haas, J.R., Shock, E.L., and Sassani, D.C., 1995. Rare earth elements in hydrothermal systems: Estimates of standard partial molal thermodynamic properties of aqueous complexes of the rare earth elements at high pressures and temperatures, Geochimica et Cosmochimica Acta, 59: 4329–4350.

Hassanpour, Sh., and Alirezaei, S., 2014. SHRIMP zircon U–Pb and biotite and hornblende Ar–Ar geochronology of Sungun, Haftcheshmeh, Kighal, and Niaz porphyry Cu–Mo systems: evidence for an early Miocene porphyry-style mineralization in northwest Iran. International Journal of Earth Sciences, 104: 45–59.

Hemley, J.J., and Hunt, J.P., 1992. Hydrothermal ore-forming processes in the light of studies in rock buffered systems; II, Some general geologic applications. Economic Geology 87: 23–43.

Jamali, H., Dilek, Y., Daliran, F., Yaghubpur, AM., and Mehrabi, B., 2010. Metallogeny and tectonic evolution of the Cenozoic Ahar–Arasbaran volcanic belt, northern Iran. International Geology Reviews, 52: 608–630.

Jankovi´c, S., 1997. The Carpatho-Balkanides and adjacent area: A sector of the Tethyan Eurasian metallogenic belt. Mineral Deposita, 32: 426–433.

Kadir, S., Külah, T., Eren, M., Önalgil, N., and Gürel, A., 2014. Mineralogical and geochemical characteristics and genesis of the Güzelyurt alunite–bearing kaolinite deposit within the Late Miocene Gördeles ignimbrite, central Anatolia, Turkey. Clays and Clay Minerals, 62: 486–508.

Karakaya, N., 2009. REE and HFS element behaviour in the alteration facies of the Erenler Dag˘ ı Volcanics (Konya, Turkey) and kaolinite occurrence. Journal of Geochemical Exploration, 101: 185–208.

Lewis, A.J., Palmer, M.R., Sturchio, N.C., and Kemp, A.J., 1997. The rare earth element geochemistry of acid-sulfate and acid-sulfate-chloride geothermal systems from Yellowstone National Park, Wyoming, USA. Geochimica et Cosmochimica Acta, 61: 695–706.

Lopez, J.M.G., Bauluz, B., Fernandez-Nieto, C., and Oliete, A.Y., 2005. Factors controlling the rare element distribution in fine- grained rocks: The albian kaolinite- rich deposits of the Oliete Basin (NE Spain). Chemical Geology, 214: 1–19.

MacLean, WH., Barrett, TJ., 1993. Lithogeochemical techniques using immobile elements. Journal of Geochemical Exploration, 48: 109–133.

MacLean, WH., 1990. Mass change calculations in altered rock series. Mineral Deposits, 25: 44–49.
Mehrpartou, M., 1999. Geological map of Iran 1:100,000 series, Kaleybar. Geological Survey of Iran.
Michard, A., 1989. Rare earth element systematics in hydrothermal fluid, Geochimica et Cosmochimica Acta, 53: 745–750.
Moayed, M., 2001. Petrological investigations of Western Alborz-Azarbaijan volcano-plutonic belt pointed to Hashtjin district [PhD thesis]. University of Saheed-Beheshti 328 (in Persian).
Mollaei, H., Yaghubpur, A., and Attarm R.S., 2009. Geology and geochemistry of skarn deposits in the northern part of Ahar batholith, East Azarbaijan, NW Iran. Iranian Journal of Earth Sciences, 1(1): 15–34.
Nabavi, M., 1976. An Introduction to the Geology of Iran. Geological Survey of Iran Publication, 109 (in Persian).
Nesbitt, HW., 1979. Mobility and fractionation of rare earth elements during weathering of a granodiorite. Nature, 279: 206–210.
Parsapoor, A., Khalili, M., Mackizadeh, M. A., 2009. The behaviour of trace and rare earth elements (REE) during hydrothermal alteration in the Rangan area (Central Iran), Journal of Asian Earth Sciences, 34: 123–134.
Patino, L.C., Velbel, M.A., Price, J.R., and Wade, J.A., 2003. Trace element mobility during spheroidal weathering of basalts and andesites in Hawaii and Guatemala, Chemical Geology, 202: 343–364.
Siahcheshm, K., 2017. Mineralogy and metasomatic evolution of the Mianeh Iron skarn deposit, Norduz-Agarak border, NW Iran. Arabian Journal of Geosciences, 10(309): 1–16.
Takahashi, Y., Tada, A., and Shimizu, H., 2004. Distribution of pattern of rare earth ions between water and montmorillonite and its relation to the sorbed species of the ions, Analytical Sciences, 20: 1301–1306.
Taylor, S.R., McLennan, S.M., 1985. The continental crust: its composition and evolution. Blackwell Oxford, 312.
Van Der Weijden, C.H., and Van Der Weijden, R.D., 1995. Mobility of major and some redox – sensitive trace element and rare earth elements during weathering of four granitoids in central Protugal, Chemical Geology, 125: 149–167.
Whitney, D.L., and Evans, B.W., 2010. Abbreviations for names of rock-forming minerals. American Mineralogist, 95: 85–187.
Wood, S.A., 1990. The aqueous geochemistry of the rare earth elements and yttrium: Theoretical prediction of speciation in hydrothermal solutions to 350°C at saturation water vapor pressure. Chemical Geology, 88: 99–125.
Zimbelman, D., Rye, R., and Brieit, G., 2005. Origin of secondary sulfate minerals on active andesitic stratovolcanoes. Chemical Geology, 215: 37–60.

About the first and corresponding author

Kamal SIAHCHESHM, as an assistant professor, a tenured member at the Department of Earth Sciences, University of Tabriz, Iran. His graduate teaching experience includes several courses, in his field of expertise, such as “Geochemistry of Hydrothermal Ore Deposits”, “Fluid inclusions study” and “Geochemistry of REEs”. He is the author and coauthor of 21 ISI and ISC papers on the geology of Iran. Email: Kl_siahcheshm@tabrizu.ac.ir; phone: +98- 41-33392693; 9141004685.